Hierarchically Structured Nitrogen-doped Carbon Microspheres for Advanced Potassium Ion Batteries

Junmin Ge, Bin Wang, Jiang Zhou, Shuquan Liang, Apparao M. Rao, Bingan Lu **

Dr. J. Ge, Prof. B. Lu
School of Physics and Electronics, State Key Laboratory of Advanced Design and Manufacturing for Vehicle Body, Hunan University, Changsha 410082, P. R. China

Prof. B. Wang
Physics and Electronic Engineering Department, Xinxiang University, Xinxiang 453003, China

Prof. S. Liang, Prof. J. Zhou
School of Materials Science and Engineering, Central South University, Changsha 410083, PR China
Key Laboratory of Nonferrous Metal Materials Science and Engineering, Ministry of Education, Central South University, Changsha 410083, PR China

Prof. B. Lu
Fujian Strait Research Institute of Industrial Graphene Technologies, Quanzhou 362000, P. R. China

Prof. A. M. Rao
FAPS, FAAAS, FNAI, FMRS Associate Dean for Discovery, College of Science Founding Director, Clemson Nanomaterials Institute R. A. Bowen Professor of Physics, Clemson University, Clemson, South Carolina 29634, United States

* Corresponding email: zhou_jiang@csu.edu.cn; luba2012@hnu.edu.cn

Experiment section

1. Materials and Chemicals:

Potassium bis(fluoroslufonyl)imide (KFSI), and potassium chunks were purchased from Sigma-Aldrich. DME was purchased from BASF. Distilled water was prepared from HHitech(Hetai) purification system. All chemicals were used as received without further purification.

2. Material Synthesis

3.5 g of g-C_3N_4 powder was thoroughly mixed with 3.5 g of Zn powder by grinding the mixture in an agate mortar. The mixture was annealed in Ar at 500 °C for 1h, and then 800 °C for 4 h with a ramp rate of 2 °C min^{-1}. After removing the Zn powder through dissolution in aqueous solution of 1 M HCl, the product was washed with distilled water several times, and then dried at 60 °C in a vacuum oven. CMSs-700 and CMSs-900 were prepared using a similar pyrolysis method as CMSs-800 but at different calcination temperatures as specified.

Characterization

The morphology of the final products (referred below as active material) was elucidated using a field emission scanning electron microscope (FE-SEM, Carl Zeiss, ΣIGMA HD, Germany) and a transmission electron microscope (TEM, Titan G2 60-300). Renishaw 2000 for Raman spectra. The structure was confirmed by XRD with a Philips X'pert diffractometer, and X-ray photoelectron spectroscopy (XPS, ESCALAB 250Xi).

3. Electrochemical measurements:

The electrodes were prepared by uniformly mixing the active material (80%), Super P (10%) and PVDF (10%) in DMF to form a uniform slurry, which was then spread on a copper foil and dried overnight. The mass loading of active material is ~ 1.0 mg cm^{-2}. CMSs-800 electrodes were pre-potassiated to form the SEI through a spontaneous reaction of K metal (Sigma-Aldrich) with high concentration inorganic potassium bis(fluoroslufonyl)imide (KFSI) (Sigma-Aldrich) in Dimethoxyethane (DME) (BASF). The galvanostatic charge/discharge tests were conducted from 0.01 to 3.0 V in battery test incubator. The cyclic voltammetry (CV) measurements were conducted using an electrochemical workstation. All capacity-related calculations are based on the mass of the active materials. Full cells were assembled with CMSs-800 as the anode, PTCDA as the cathode and 3 M KFSI in DME as the electrolyte. As mentioned above, CMSs-800 is pre-potassiated prior to using them in assembled full cell. The full cells capacity-related calculations are based on total mass of the active material of the anode and cathode. The average active material loading for the cathode is 1.2 mg cm^{-2}, while that for CMSs-800 anode is 0.8 mg cm^{-2}.

4. Calculated Method and Crystal Structure:

The present calculations were performed based on the density functional theory (DFT) using the Cambridge Serial Total Energy Package (CASTEP) plane wave code. Ultrasoft pseudopotentials were used to describe the interaction of ionic core and valence electrons. Valence states corresponding to $C2s^22p^2$, $N2s^22p^3$ and $K3s^2p^64s^1$ were considered in this study. The generalized gradient approximation

(GGA) of Perdew–Burke–Ernzerh method parameterized by Perdew was used to calculate the exchange and correlation terms. Brillouin-zone integrations were performed using Monkhorst and Pack k-point meshes. During the calculation, the 310 eV for cutoff energies and 3×3×3 for the numbers of k-point ensured convergence of the total energy. All the calculations were considered converged when the maximum force on the atom was below 0.01eVÅ^{-1}, maximum stress was below 0.02GPa, and the maximum displacement between cycles was below 0.0005 Å.

In the calculations, a 4x4x1 supercell with periodic structure was used. The structures are shown in Figure S9a. Graphite (G) belongs to the space group of P63/MMC and 62 atoms are contained in the supercell. Two C atoms are deleted in the middle of the honeycomb lattice as shown in Figure S9b (G_d). After geometry optimization, the resulting lattice parameters are listed in Table S2 and compared with other experimental data reported in the literature. From Table S2, it is inferred that the calculated data are close to the experimentally determined values. Furthermore, the volume of G_d decreased little compared to the volume of G.

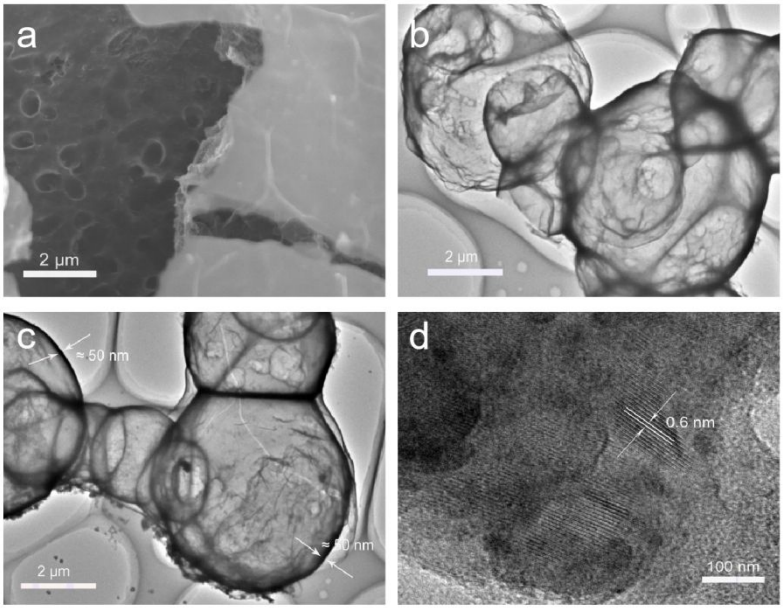

Figure S1. The TEM images of CMSs-800.

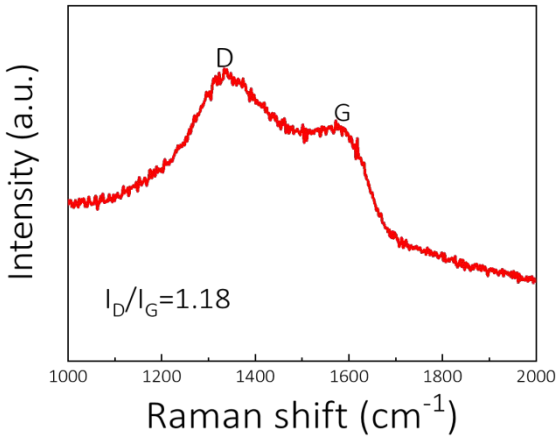

Figure S2. The Raman spectrum of CMSs-800.

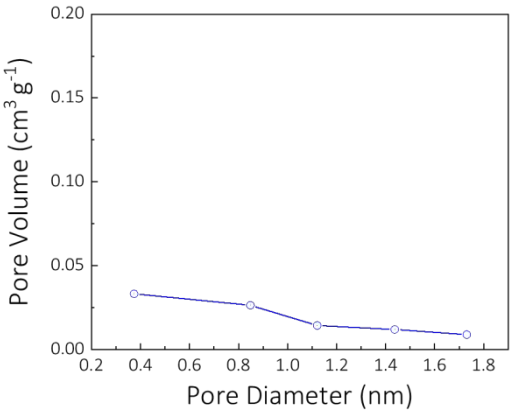

Figure S3. The pore size distribution of CMSs-800 calculated from the adsorption isotherms using the BET method.

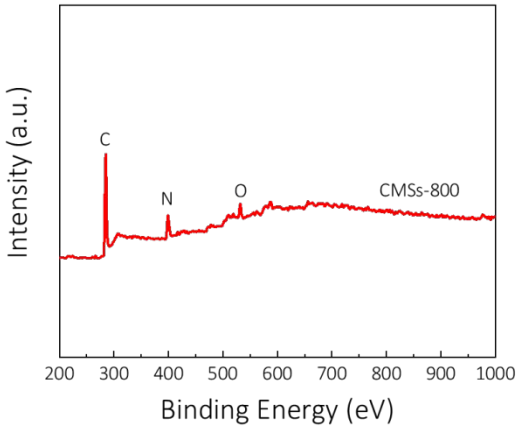

Figure S4. XPS survey spectra of CMSs-800.

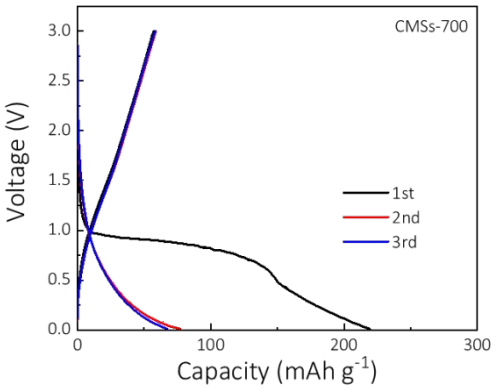

Figure S5. The discharge/charge curves of CMSs-700.

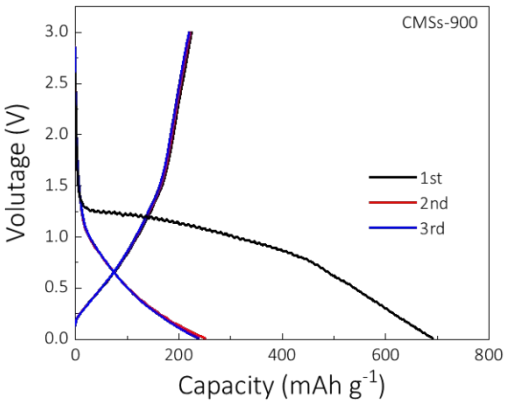

Figure S6. The discharge/charge curves of CMSs-900.

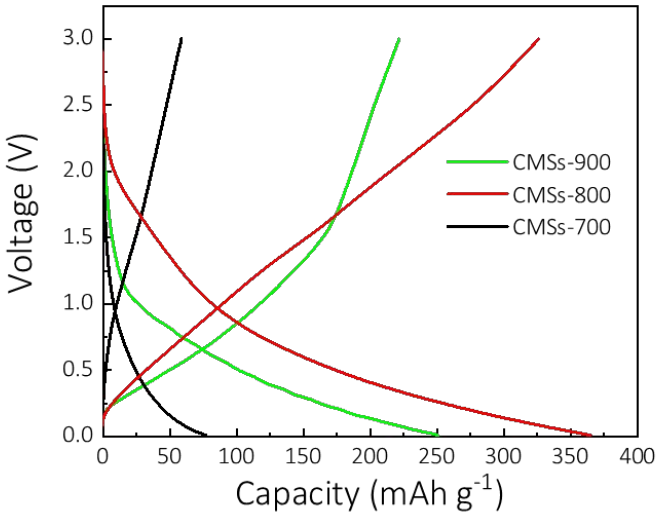

Figure S7. Comparison of discharge/charge curves of the CMSs prepared at different calcination temperatures.

Table S1. Comparison of the electrochemical cycle stability of CMSs-800 electrodes with other carbon based electrodes for PIBs reported in the recently published literature.

Ref.	Sample	Cycle number	Specific capacity
This work	CMSs-800	1000 10000	257 mAh g^{-1} at 0.1 A g^{-1} 136 mAh g^{-1} at 2 A g^{-1}
[1]	WPCSs	240 3000	257 mAh g^{-1} at 0.2 A g^{-1} 135 mAh g^{-1} at 2 A g^{-1}
[2]	3DNFC	1000	137 mAh g^{-1} at 2 A g^{-1}
[3]	NOHCs-800	1000	189 mAh g^{-1} at 1 A g^{-1}
[4]	CNS-700	1300 3000	147 mAh g^{-1} at 2 A g^{-1} 111 mAh g^{-1} at 5 A g^{-1}
[5]	NCNF-650	1000 2000 4000	205 mAh g^{-1} at 0.5 A g^{-1} 164 mAh g^{-1} at 1 A g^{-1} 146 mAh g^{-1} at 2 A g^{-1}
[6]	N-NCS	5500	321 mAh g^{-1} at 5 A g^{-1}

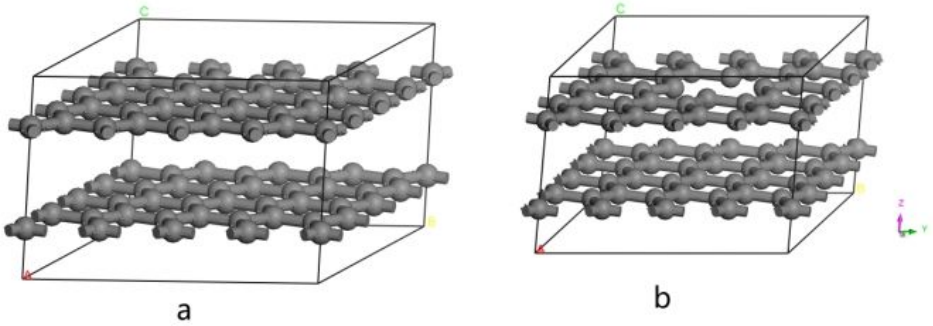

Figure S8. a. 4x4x1 supercell structure of graphite. b. 4x4x1 supercell structure of graphite without the two atoms in the middle of the honeycomb lattice.

Table S2

Calculated equilibrium lattice parameters (*a* and *c*) and volume (*V*) of graphite (G) and defective graphite (G_d) compared with experimental data.

	a(Å)	*c*(Å)	*V*(Å^3)
G	9.85	6.69	561.94
Expt.[7]	10.4	6.71	628.505
Expt.[8]	9.84	6.71	562.64
G_d	9.81	6.74	553.35

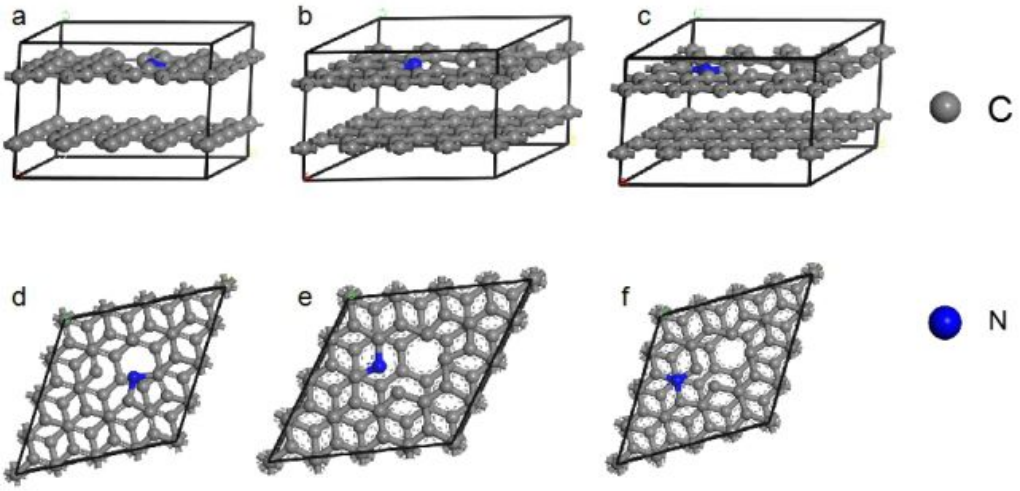

Figure S9. Theoretical simulations of different N-doped structures. Side view of the N-5 (a), N-Q (b), and N-6 (c) structures and the top view of N-5 (d), N-Q (e), and N-6 (f) structures.

Table S3

Calculated equilibrium lattice parameters (*a* and *c*), volume (*V*) and layer distance (L_d) of defective graphite (G_d), N-5, N-6, N-Q; and with one K atom inserted in N-5, N-6, N-Q. Energies (E_i) for inserting one K atom in N-5, N-6, N-Q are also calculated.

	a(Å)	*c*(Å)	*V*(Å^3)	L_d(Å)	E_i
G_d	9.81	6.74	553.35	3.37	-
G_{N-5}	9.78	6.72	560.42	3.36	-
G_{N-6}	9.81	6.73	551.22	3.39	-
G_{N-Q}	9.80	6.73	550.40	3.37	-
G_{N-5}+K	9.79	8.18	682.45	4.29	-3.14
G_{N-6}+K	9.81	8.02	660.73	4.71	-2.97
G_{N-Q}+K	9.81	8.50	696.89	5.08	-2.53

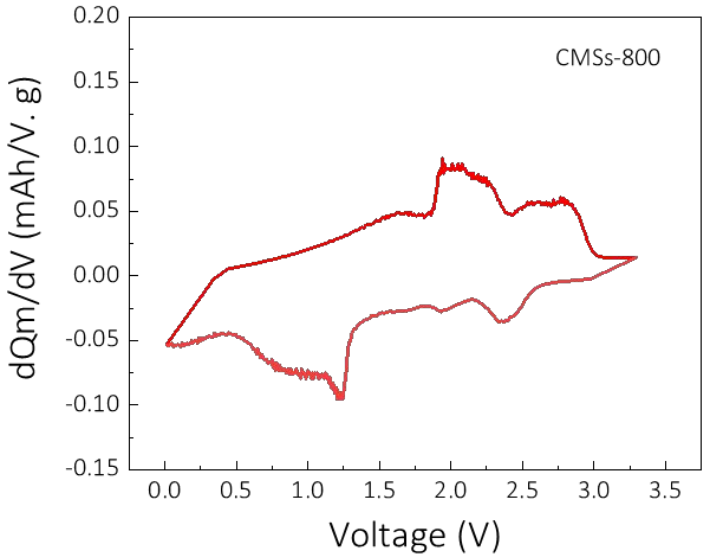

Figure S10. The dQm/dV curves of full cell.

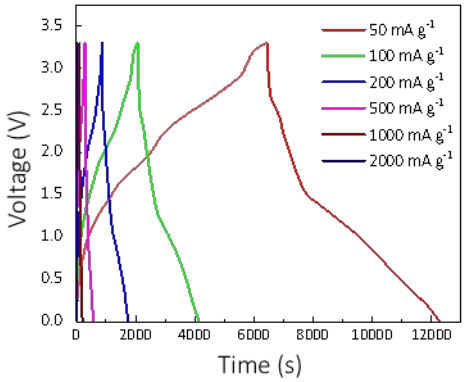

Figure S11. GCD profiles of CMSs-800//PTCDA full cell.

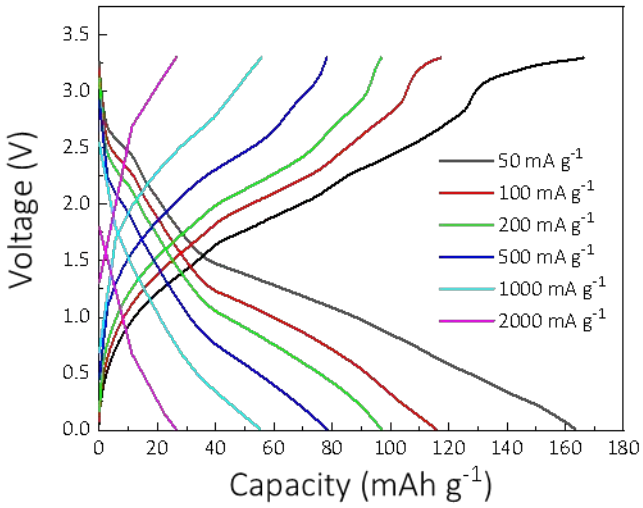

Figure S12. The charge/discharge curves of full cell at different current densities.

[1] Y. Cui, W. Liu, X. Wang, J. Li, Y. Zhang, Y. Du, S. Liu, H. Wang, W. Feng, M. Chen, *ACS Nano* **2019**, *13*, 11582.
[2] B. Yang, J. Chen, L. Liu, P. Ma, B. Liu, J. Lang, Y. Tang, X. Yan, *Energy Storage Materials* **2019**, *10.1016/j.ensm.2019.04.008*.
[3] R. C. Cui, B. Xu, H. J. Dong, C. C. Yang, Q. Jiang, *Advanced Science* **2020**, 1902547.
[4] J. Chen, B. Yang, H. Hou, H. Li, L. Liu, L. Zhang, X. Yan, *Adv. Energy Mater.* **2019**, *9*, 1803894.
[5] Y. Xu, C. Zhang, M. Zhou, Q. Fu, C. Zhao, M. Wu, Y. Lei, *Nat Commun* **2018**, *9*, 1720.
[6] H. Huang, R. Xu, Y. Feng, S. Zeng, Y. Jiang, H. Wang, W. Luo, Y. Yu, *Adv Mater* **2020**, e1904320.
[7] Hanfland M, Beister H, Syassen K, "Graphite under pressure: Equation of state and first-order Raman modes," Physical Review B, V. 39, No. 17. **1989**, pp. 12598-603
[8] Zhao YX, Spain IL, "X-ray diffraction data for graphite to 20 GPa," Physical Review B, V. 40, No. 2. **1989**, pp. 993-7